ISSN 0021-3640, JETP Letters, 2020, Vol. 111, No. 10, pp. 539–542. © Pleiades Publishing, Inc., 2020.
Russian Text © The Author(s), 2020, published in Pis'ma v Zhurnal Eksperimental'noi i Teoreticheskoi Fiziki, 2020, Vol. 111, No. 10, pp. 641–645.

OPTICS
AND LASER PHYSICS

Response of a SINIS Detector with Electron Cooling to Submillimeter-Wave Radiation

A. A. Gunbina[a, b], S. A. Lemzyakov[c, d], M. A. Tarasov[e], V. S. Edelman[c, *], and R. A. Yusupov[e]

[a] *Institute of Applied Physics, Russian Academy of Sciences, Nizhny Novgorod, 603950 Russia*
[b] *Nizhny Novgorod Technical State University named after R.E. Alekseev, Nizhny Novgorod, 603950 Russia*
[c] *Kapitza Institute for Physical Problems, Russian Academy of Sciences, Moscow, 119334 Russia*
[d] *Moscow Institute for Physics and Technology (National Research University), Dolgoprudnyi, Moscow region, 141701 Russia*
[e] *Kotelnikov Institute of Radio Engineering and Electronics, Russian Academy of Sciences, Moscow, 125009 Russia*
**e-mail: vsedelman@yandex.ru*

Received March 29, 2020; revised April 16, 2020; accepted April 16, 2020

The response of a detector fabricated on a silicon substrate in the form of a metamaterial that is a 10 × 10 matrix of split rings containing superconductor–insulator–normal metal–insulator–superconductor tunnel structures to submillimeter wave radiation has been experimentally studied. At voltages below the superconducting gap, the electron temperature T_e at the substrate temperature $T \sim 0.1$ K is ~0.23 K due to overheating by spurious radiation. At the substrate temperature $T \sim 0.3$ K, the electron temperature is close to the substrate temperature $T_e \approx T$. In both cases, with increasing voltage, T_e decreases due to electron cooling and reaches 0.19 K at a voltage corresponding to the maximum response. The response at $T = 0.1$ K is greater than that at $T \sim 0.3$ K by a factor of 5–6. Thus, cooling of only electrons does not provide the same responsivity as cooling of the detector as a whole.

DOI: 10.1134/S0021364020100094

A characteristic feature of tunneling structures of the type superconductor–insulator–normal metal–insulator–superconductor (SINIS) is the cooling effect of a normal metal electrode N when current flow. It is caused by the fact that when the bias voltage at the NIS junction is lower than the energy gap $V_{gap} = k\Delta_c/e$ (Δ_c [K] is the energy gap of the superconductor), the current is provided by the highest-energy electrons. As a result, a heat flux transfers from a normal metal to a superconductor. In this case, the total power, which consists of the Joule heating IU and the power of electronic cooling, is dissipated in superconducting elements and leads to their overheating relative to the cold substrate. It partially transfers to a normal metal due to backward tunneling and phonon transport, and often can be less than the cooling power. In this case, the electron temperature of the normal metal T_e can become lower than the temperature of the substrate.

The authors of [1] mention that electron cooling in SINIS structures may be useful for detecting terahertz radiation, because the sensitivity of such detectors is higher if the temperature is lower. Subsequently, this idea was often presented as a way to achieve the ultimate sensitivity of detectors using the relatively simple technology of cooling by pumping liquid ^{3}He rather than more complex and expensive methods like dilution refrigeration (see, e.g., [2, 3] and references therein).

However, cooling an electronic system is not equivalent to cooling a sample as a whole. For example, in [3] the phonon temperature T_{ph} changes little during electron cooling. In [3], the rate of energy exchange between electrons and phonons is described by the expression $P_{e-ph} = \Sigma v(T_e^5 - T_{ph}^5)$, where Σ is the interaction constant and v is the sample volume. Therefore, e.g., at $T \sim 0.3$ K, when the electron temperature is halved, the heat transfer is determined by the phonon temperature, and at bath temperature $T \sim 0.1$ K, the heat transfer will be determined by the higher electron temperature, and the response will vary greatly.

Another feature that radically differs the SINIS operation as a terahertz radiation detector from a bolometer operation detecting the heating at a constant or relatively low-frequency current is a significant excess of the radiation energy quantum $\hbar\omega$ over kT. For example, at a frequency of 350 GHz, corresponding to one of the transparency windows of the Earth's atmosphere, $\hbar\omega/k \approx 17$ K. As mentioned in [4], the electrons absorbing such photons, on average, acquire an equivalent thermal energy of about 8–9 K, and then a complex multistage relaxation process occurs with the emission and absorption of phonons

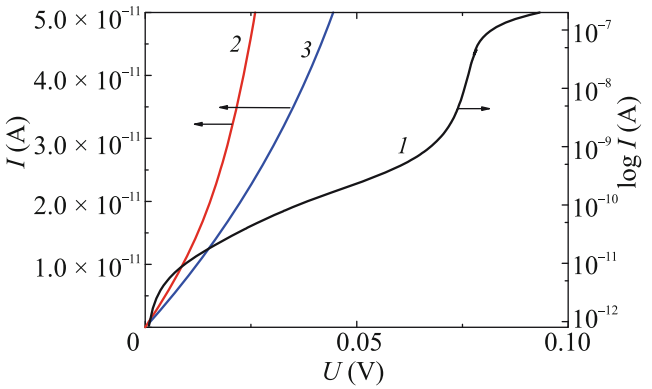

Fig. 1. (Color online) (*1*) Current–voltage characteristic of the metastructure at $T = (0.095 \pm 0.01)$ K in the logarithmic scale, (*2*) its initial section at low voltages, and (*3*) the calculated Andreev current.

and with electron–electron interaction. It begins with the very fast creation of high-energy phonons and continues with more and more slow processes. In this case, characteristic times even at particle energies of the order of 2 K are comparable with a tunneling time of the order of a dozen nanoseconds and high-energy electrons leave the normal metal before the state described by the Fermi distribution with temperature T_e established in the electronic system. As shown in [4], the maximum response is achieved when the resistance of NIS junctions with an area of 1 μm^2 is about 10 kΩ, which is an order of magnitude higher than the resistance of commonly studied structures exhibiting electron cooling. A lack of equilibrium in the electronic system during the irradiation of the SINIS detector at a frequency of ≈350 GHz observed in [5].

The experiments described below demonstrate the difference between the SINIS response of terahertz radiation detectors at the same electron temperature, but at different sample temperatures. The measurements carried out with a planar receiving structure made of metamaterial on a silicon chip [6], which is a 10 × 10 matrix of identical antennas connected in series for direct current. Each element is a split-ring aluminum antenna with an external diameter of 54 μm, with SINIS elements in each of four breaks. The matrix area is 0.38 mm^2. The structure of the tunnel junctions consists of lower normal electrode of aluminum with a thickness of 14 nm on an iron sublayer of 1.2 nm, which suppresses superconductivity, tunnel barrier, and top superconducting aluminum electrode. An aluminum oxide film with a thickness of about 1 nm serves as a tunnel barrier between a normal and superconducting aluminum layer with a thickness of 80 nm. The area of each tunnel junction is 1 μm^2, and the absorber strip between the normal layers in the SINIS structure has sizes 1 × 0.1 μm. The normal resistance r_n of single junctions is 1.15 kΩ, the total resistance of the structure is R_n = 230 kΩ. Compared to detectors with a small number of elements with bias voltage about hundreds of microvolts, the voltage across a multi-element structure reaches tens of millivolts. Because of this, the signal to noise ratio in array is much larger than that of single SINIS, which is important both in measuring the response, especially at a relatively high temperature, and in calculating the electron temperature for a normal electrode in which radiation is absorbed.

In measurements, we use data acquisition system with NI USB 6289 ADC/DAC I/O board. Samples were current biased via series resistors connected to DAC voltage output. The voltage across the structure was amplified by two orders of magnitude by an instrumental amplifier operating at room temperature, and digitized with ADC. Measurements carried out at chip temperatures of 0.09–0.5 K using a dilution microcryostat [7].

The response to electromagnetic radiation was measured using a black body radiation source, which was a current-heated NiCr film with a resistance of about 300 Ω/□ deposited on a sapphire substrate 0.3 mm thick. The current to this source was applied through copper wires with a diameter of 0.02 mm and a length of ~1 cm, with which it was attached to a holder at a temperature of 0.4–0.5 K. We heat the film up to 7–8 K with applied power of tens of microwatts without significant influence on the operation of cryostat.

The I–V curve measured with a "cold" source at a chip temperature $T = 0.095$ K is shown in Fig. 1. The dynamic resistance corresponding to this I–V curve is $R_d(U = 0) = 920$ MΩ and $R_d(U = 0)/R_n = 4000$. With such a large resistance ratio, as a rule, the Andreev current appears, exceeding the single-electron tunneling current [8]. As was found in the cited paper, for NIS transitions with suppression of the normal electrode superconductivity by the magnetic sublayer, only that component of the Andreev current retained, which is due to the diffusion motion of excitations in the superconducting electrode. At low voltages far from the gap, it has the form, according to [9]:

$$I_s = K_s \frac{eU/k\Delta_c}{\sqrt{1 - eU/k\Delta_c}}.$$

The electron temperature T_e of normal elements is determined by the single-electron current. In order to extract electron temperature from the total current of the experimental I–V characteristic, the Andreev contribution subtracted by choosing the coefficient K_s so that T_e varies insignificantly at low voltages. This obvious requirement is because at low voltages, both heating and cooling are low and cannot significantly affect the temperature. Actually, the Andreev current was found to be needed to account at voltages less than $(0.2–0.3)k\Delta_c/e$, since its contribution is negligible at higher voltages. The temperature T_e is calculated

according to the well-known formula of the tunnel theory for a single-particle current given in [10, 11]:

$$I = \frac{1}{eR_n}\int_{-\infty}^{+\infty} N_S(E)[n_N(E - eU) - n_S(E)]dE.$$

Here, R_n is the normal resistance of the junction, $N_S(E) = \frac{|E|\Theta(|E| - k\Delta_c)}{\sqrt{E^2 - (k\Delta_c)^2}}$ is the density of states in the superconductor according to the BCS theory, and $n_N(E, T_e)$ and $n_S(E, T_S)$ are the Fermi distribution functions in the normal metal and superconductor, respectively. The above formula formally includes the temperature of the superconductor, but symmetrizing the integrand, we obtain the following more convenient formula that does not contain terms that depend on the temperature of the superconductor [12]:

$$I = \frac{1}{eR_n}\int_{0}^{+\infty} N_S(E)[n_N(E - eU) - n_N(E + eU)]dE.$$

For each point of the measured current–voltage characteristic, the electron temperature T_e calculated using numerical integration so that the difference between the measured current and the value of the expression on the right side of this formula did not differ by more than a hundredth of a percent, which obviously exceeds the measurement accuracy. It is important to note that the electron temperature value generally depends on the parameters of junction. Moreover, if for low bias voltages this influence is relatively weak, then for voltages close to $V_{gap} = k\Delta_c/e$ it is significant. For matrix structures, the situation is more complicated due to the presence of a small spread in the parameters for different junctions, which is confirmed by the smearing of the minimum of the differential resistance. Therefore, the calculation results near the gap ($U > 0.8k\Delta_c$) can be significantly distorted. In addition, in general, the results of calculating electron temperatures should be treated with caution, since the calculations are based on the assumption of equilibrium of the electronic system, i.e., described by the Fermi function of the electron energy distribution. As noted above, when irradiated with high-energy photons, this condition is not guaranteed.

The results of calculating T_e from the I–V characteristics measured at chip temperatures T of 0.095 and 0.316 K with radiation source "cold" and heated to 7.05 K are shown in Fig. 2. The voltage dependences of temperature changes $T_e - T$ under the influence of radiation also given there. As follows from the above results, at $T = 0.095$ K, the electron temperature at $U \ll V_{gap}$ is significantly higher than this value of bath temperature. Such a difference usually observed for SINIS detectors and, apparently, this is due to spurious room-temperature radiation [13]. With additional irradiation from a heated source, T_e increases noticeably. With an increase in voltage in all of Fig. 2 cases,

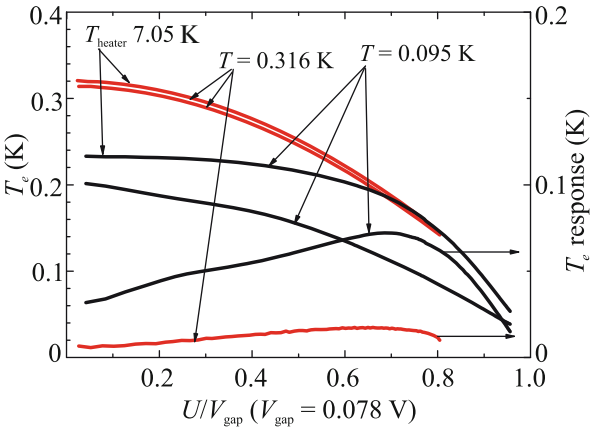

Fig. 2. Calculated voltage dependences of T_e and $T_e - T$ at two temperatures $T = (0.095 \pm 0.01)$ K and $T = (0.316 \pm 0.02)$ K with a cold radiation source and a source heated to (7.05 ± 0.1) K.

electron cooling observed. Note that the radiation-induced increase in the electron temperature at 0.095 K at low voltages is about five times higher than that at 0.316 K. This, in order of magnitude, corresponds to the expected ratio of temperature responses during electron–phonon interaction, when for the same absorbed power it can be expected that $\delta T_e(T = 0.095\text{ K})/\delta T_e(T = 0.316\text{ K}) \approx (0.316/0.2)^4 \approx 6$.

Figure 3 shows the voltage, $U(I, T_{heater} \approx 0.5\text{ K}) - U(I, T_{heater} = 7.05\text{ K})$, and current, $I(U, T_{heater} = 7.05\text{ K}) - I(U, T_{heater} \approx 0.5\text{ K})$, responses extracted directly from the measured I–V characteristics. It can be seen that the voltage response at both bath temperatures 0.095 and 0.316 K is maximum at a reduced voltage of about 0.65, when the electron temperatures are almost equal. Moreover, at $T = 0.095$ K, it is 5.3 times larger than at 0.316 K. The current response is slightly greater at higher temperatures. But this advantage is ephemeral from a practical point of view, since the current itself at this temperature is an order of magnitude larger and the contribution of its fluctuations to noise is three times greater than at $T = 0.095$ K. In addition, phonon noise is also correspondingly larger.

For comparison with the results of [3], we use the method proposed in it for estimating the radiation power P_{rad} absorbed by the receiving structure based on the heat balance equation, which for $U \ll V_{gap}$ has the form $P_0 + P_{rad} = \Sigma v(T_e^5 - T_{ph}^5)$, where P_0 is the spurious room-temperature radiation. If the temperature change due to radiation is small, then this expression reduces to $P_{rad} = 5\Sigma v T_e^4 \delta T_e$. Considering that in this work the construction of SINIS elements is similar to those used in our work, we use the value $\Sigma = 1.3\text{ nW K}^{-5}\,\mu\text{m}^{-3}$ from [3]. Then, at a temperature

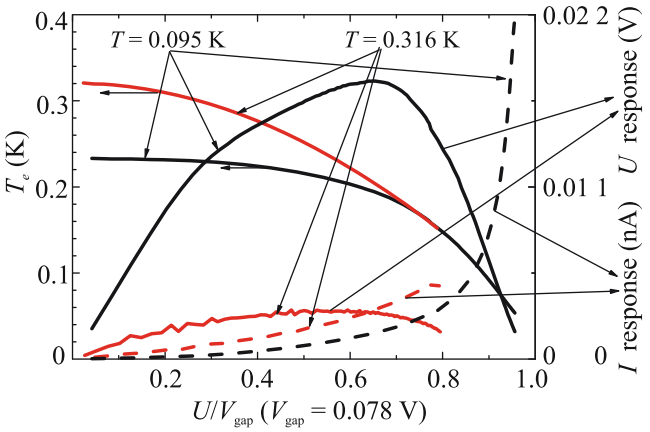

Fig. 3. Voltage dependences of the electron temperature in the detector normal absorbers (left scale) and of the voltage and current responses (right scale) at temperatures of (0.095 ± 0.01) K and (0.316 ± 0.02) K when irradiated from a source heated to (7.05 ± 0.1) K.

of 0.095 K and at $\delta T_e \ll T_e$, we obtain $P \approx 0.01$ pW for one NIS, and for the entire structure containing 800 NIS, we obtain (4 ± 0.4) pW. According to Fig. 3, the maximum radiation response is 4×10^9 V/W, which is 5 times greater than that at approximately the same power absorbed by the detector, but given at [3] at a substrate temperature of 0.2 K.

Thus, a direct experiment disproves expectations of avoiding of lowering the real temperature of the SINIS detector to achieve the ultimate responsivity. Replacing dilution cryostats with ^{3}He evacuation cryostats is not critical, given the possibility of constructing autonomous compact solution microcryostats [7].

ACKNOWLEDGMENTS

The samples were fabricated and studied using the unique scientific setup UNU no. 352529.

FUNDING

This work was supported by the Ministry of Science and Higher Education of the Russian Federation (state assignment nos. 0027-2019-0003 and 0030-2019-0003 for Kapitza Institute for Physical Problems and Kotelnikov Institute of Radio Engineering and Electronics, respectively).

REFERENCES

1. L. S. Kuzmin, I. A. Devyatov, and D. Golubev, in *Millimeter and Submillimeter Waves IV,* Proc. SPIE **3465**, 193 (1998).
2. L. S. Kuz'min, Phys. Usp. **48**, 519 (2005).
3. L. S. Kuzmin, A. L. Pankratov, A. V. Gordeeva, V. O. Zbrozhek, V. A. Shamporov, L. S. Revin, A. V. Blagodatkin, S. Masi, and P. de Bernardis, Commun. Phys. **2**, 104 (2019).
4. I. A. Devyatov, P. A. Krutitski, and M. Yu. Kupriyanov, JETP Lett. **84**, 57 (2006).
5. M. A. Tarasov, V. S. Edel'man, S. Mahashabde, and L. K. Kuzmin, J. Exp. Theor. Phys. **119**, 107 (2014).
6. M. Tarasov, A. Sobolev, A. Gunbina, G. Yakopov, A. Chekushkin, R. Yusupov, S. Lemzyakov, V. Vdovin, and V. Edelman, J. Appl. Phys. **125**, 174501 (2019).
7. V. S. Edelman, Instrum. Exp. Tech. **52**, 301 (2009).
8. A. V. Seliverstov, M. A. Tarasov, and V. S. Edel'man, J. Exp. Theor. Phys. **124**, 643 (2017).
9. F. W. J. Hekking and Yu. V. Nazarov, Phys. Rev. B **49**, 6847 (1994).
10. I. Giaever and K. Megerle, Phys. Rev. **122**, 1101 (1961).
11. A. S. Vasenko, E. V. Bezuglyi, H. Courtois, and F. W. Hekking, Phys. Rev. B **81**, 094513 (2010).
12. F. Giazotto, T. T. Heikkilä, A. Luukanen, A. M. Savin, and J. P. Pekola, Rev. Mod. Phys. **78**, 217 (2006).
13. A. Di Marko, V. F. Maisi, J. P. Pekola, and J. Hekking, Phys. Rev. B **88**, 174507 (2013).

Translated by the authors